

*Supplementary Information*

**Functional ligands directed assembly and electronic structure of Sn<sub>18</sub>-oxo wheel nanocluster**

Yu Zhu,<sup>+ a, b</sup> Qiaohong Li,<sup>+ a</sup> Dongsheng Li,<sup>b</sup> Jian Zhang<sup>a</sup> and Lei Zhang<sup>a\*</sup>

<sup>a</sup>State Key Laboratory of Structural Chemistry, Fujian Institute of Research on the Structure of Matter, Chinese Academy of Sciences, Fuzhou 350002, P.R. China.

<sup>b</sup>Key Laboratory of Inorganic Nonmetallic Crystalline and Energy Conversion Materials, College of Materials and Chemical Engineering, China Three Gorges University, Yichang 443002, P. R. China.

<sup>+</sup>These authors contributed equally to this work and should be considered co-first authors.

E-mails: [LZhang@fjirsm.ac.cn](mailto:LZhang@fjirsm.ac.cn)

## Experimental Section

### Materials and Instrumentation.

All the chemical reagents were commercially purchased and used without further purification. IR spectrum was obtained on a Vertex 7.0 spectrometer equipped with attenuated total reflectance (ATR) measurements. Powder XRD pattern was obtained by using a Miniflex600 diffractometer with CuK $\alpha$  radiation ( $\lambda = 1.54056 \text{ \AA}$ ). Elemental analyses (C, H, and N) were performed on a vario MICRO elemental analyzer. ESI-MS was carried out on Impact II UHR-TOF (Bruker). The  $^1\text{H}$  NMR spectrum was measured on the Bruker AVANCE III spectrometer (400MHz).

**Synthesis of TOC-9:** Butyltin hydroxide oxide (208.8 mg, 1.0 mmol), 3, 5-dihydroxybenzoic acid (154.1 mg, 1.0 mmol), acetonitrile (5 mL) were mixed and sealed in a 20 mL vial, then transferred to a preheated oven at 80 °C for 5 days, and cooling crystallized at room temperature to obtain the colorless crystals (yield: 5 % based on Sn). In addition, the yield of the **TOC-9** can be improved to some extent by adding NaOH (10 mg) to this reaction, but the obtained crystals become smaller. Anal. calcd for  $\text{Sn}_{18}\text{O}_{91}\text{C}_{170}\text{H}_{262}$  (%): C, 34.61; H, 4.44. Found: C, 34.31; H, 4.42.

### Computational Methods

**DFT calculations.** The initial geometric structures of the **Sn<sub>18</sub>** wheel cluster were taken from the X-ray diffraction data. The butyl groups of **Sn<sub>18</sub>** are replaced by the methyl groups to simplify the theoretical calculation. The molecular geometries were fully optimized to the local energy minima, which have been confirmed by no imaginary harmonic vibration frequency. All the calculations were using Gaussian 16.<sup>[1]</sup> The ground-state equilibrium geometries of **Sn<sub>18</sub>** cluster were fully optimized

using B3LYP functional and 6-31g(d, p) basis sets for C, H, and Lan12DZ basis set for metal atoms, with D3 dispersion correction of Grimme,<sup>[2-9]</sup> The frequency-dependent NLO response is calculated by the complete summation sum-over-states (SOS) method. TDDFT and the static third-order nonlinear polarizability calculations of the **Sn**<sub>18</sub> cluster were used cam-B3LYP<sup>[10]</sup> and 6-31+g(d, p) basis sets for C, H. In order to get a deeper understanding of the wave function, Multiwfn<sup>[11]</sup> and VMD<sup>[12]</sup> software was used to analyse the electronic structures, excitation characteristics and (hyper)polarizability. The SOS method<sup>[13]</sup> is a common method of NLO calculation. Static hyperpolarizabilities can be calculated from the energy of each excited state and the transition dipole moment between each excited state. As shown in the following formula:

$$\beta_{ABC}(-\omega_\sigma; \omega_1, \omega_2) = \hat{P} [A(-\omega_\sigma), B(\omega_1), C(\omega_2)] \sum_{i \neq 0} \sum_{j \neq 0} \frac{\mu_{0i}^A \overline{\mu_{ij}^B} \mu_{j0}^C}{(\Delta_i - \omega_\sigma)(\Delta_j - \omega_2)}$$

$$\gamma_{ABCD}(-\omega_\sigma; \omega_1, \omega_2, \omega_3) = \hat{P} [A(-\omega_\sigma), B(\omega_1), C(\omega_2), D(\omega_3)] (\gamma^I - \gamma^{II})$$

$$\gamma^I = \sum_{i \neq 0} \sum_{j \neq 0} \sum_{k \neq 0} \frac{\mu_{0i}^A \overline{\mu_{ij}^B} \overline{\mu_{jk}^C} \mu_{k0}^D}{(\Delta_i - \omega_\sigma)(\Delta_j - \omega_2 - \omega_3)(\Delta_k - \omega_3)}$$

$$\gamma^{II} = \sum_{i \neq 0} \sum_{j \neq 0} \frac{\mu_{0i}^A \mu_{i0}^B \mu_{0j}^C \mu_{j0}^D}{(\Delta_i - \omega_\sigma)(\Delta_i - \omega_1)(\Delta_j - \omega_3)}$$

A,B,C..., and so on denote one of directions;  $\omega$  is energy of external fields;  $\Delta_i$  stands for excitation energy of state  $i$  with respect to ground state 0;  $\mu_{ij}^A$  is a component of transition dipole moment between state  $i$  and  $j$ .

We used the magnitude of hyperpolarizability to quantitatively study the nonlinear polarizability of the system.

$$\beta_i = (1/3) \sum_j (\beta_{ijj} + \beta_{jji} + \beta_{jij}) \quad i, j = \{x, y, z\}$$

$$\beta_{tot} = \sqrt{\beta_x^2 + \beta_y^2 + \beta_z^2}$$

The  $i$  components of  $\gamma$  are defined as

$$\gamma_i = (1/15) \sum_j (\gamma_{iji} + \gamma_{ijj} + \gamma_{ijj}) \hat{i}, j = \{x, y, z\}$$

The total magnitude of  $\gamma$  is measured as

$$\gamma_{tot} = \sqrt{\gamma_x^2 + \gamma_y^2 + \gamma_z^2}$$

The second and third nonlinear optical polarizability density along the backbone was calculated. The contrast between the dipole moment after Taylor expansion and electron density gives the hyperpolarizability of oligomer unit as follow:

$$\mu(F) = - \frac{\partial E}{\partial F} = \mu_0 + \alpha F + (1/2) \beta F^2 + (1/6) \gamma F^3 + \dots$$

$$\rho(r, F) = \rho^{(0)}(r) + \rho^{(1)}(r)F + (1/2) \rho^{(2)}(r)F^2 + (1/6) \rho^{(3)}(r)F^3 + \dots$$

$$\gamma_{xxx} = \int -\rho_{xxx}^{(3)}(r) x dr$$

$$\rho_{xxx}^{(3)} = \frac{\rho(2F^x) - 2\rho(F^x) + 2\rho(-F^x) - \rho(-2F^x)}{2(F^x)^3}$$

### X-ray Crystallography:

X-ray diffraction data of compound **TOC-9** was collected on a MM007-Saturn724+ diffractometer with graphite-monochromated MoK $\alpha$  ( $\lambda = 0.71073 \text{ \AA}$ ) radiation. The program SADABS was used for absorption correction. The structure was solved by direct methods and refined on  $F^2$  by full-matrix least-squares methods with the SHELX 2016 program package.<sup>[14]</sup> The intensity of diffraction for **TOC-9** is weak at high angles. Some disordered solvent molecules of **TOC-9** are not identified in the structure, and are removed by using the SQUEEZE routine of PLATON.<sup>[15]</sup> The details of the SQUEEZE corrections, including the volume of void space and electron counts, are provided in the cif file. The numbers of disordered solvent molecules of **TOC-9** are determined by the elemental analysis. CCDC 2055071 contains the supplementary crystallographic data for this paper.

**Table S1.** Crystal data collection and refinement details for **TOC-9**.

Compound	<b>TOC-9</b>
Formula	Sn <sub>18</sub> O <sub>91</sub> C <sub>170</sub> H <sub>262</sub>
Fw	5898.20
Crystal system	Orthorhombic
space group	<i>Pmna</i>
<i>a</i> /Å	27.106(6)
<i>b</i> /Å	15.460(3)
<i>c</i> /Å	46.953(10)
<i>a</i> /deg.	90
<i>β</i> /deg	90
<i>γ</i> /deg	90
<i>V</i> /Å <sup>3</sup>	19676(7)
<i>Z</i>	2
<i>D<sub>c</sub></i> /mg·m <sup>-3</sup>	0.996
<i>F</i> (000)	5820
<i>T</i> /K	293(2)
<i>μ</i> /mm <sup>-1</sup>	1.169
<i>θ</i> range /°	2.045-27.486
Reflections collected	122013
Independent reflections	22601
GOF ( <i>F</i> <sup>2</sup> )	1.096
<i>R</i> <sub>1</sub> / <i>wR</i> <sub>2</sub> [ <i>I</i> > 2σ ( <i>I</i> )]	0.0687/0.1977
<i>R</i> <sub>1</sub> / <i>wR</i> <sub>2</sub> <sup>[a]</sup> (all data)	0.0871/0.2155

$$^a R_1 = \frac{\sum ||F_o| - |F_c||}{\sum |F_o|}, wR_2 = \left[ \frac{\sum w(F_o^2 - F_c^2)^2}{\sum w(F_o^2)} \right]^{1/2}.$$

**Table S2.** Bond valence sum calculations<sup>[a]</sup> of μ<sub>3</sub>-O atoms in asymmetric unit of **TOC-9**.

<b>O21.836</b> Sn1-O2 0.665 d=2.056(5) Sn2-O2 0.582 d=2.105(3) Sn1-O2#1 0.589 d=2.101(3)	<b>O3 1.869</b> Sn1-O3 0.628 d=2.077(3) Sn2-O3 0.625 d=2.079(5) Sn5-O3 0.616 d=2.084(4)	<b>O4 1.754</b> Sn3-O4 0.602 d=2.093(7) Sn4-O4 0.576 d=2.109(2) Sn4-O4 0.576 d=2.109(2)
<b>O5 1.977</b> Sn4-O5 0.647 d=2.066(4) Sn5-O5 0.628 d=2.077(5) Sn2-O5 0.702 d=2.036(4)	<b>O6 1.929</b> Sn3-O6 0.640 d=2.070(3) Sn4-O6 0.620 d=2.082(5) Sn5-O6 0.669 d=2.054(4)	

Symmetry transformations used to generate equivalent atoms: #1 x, -y, -z.

$^{[a]}V_i = \sum_j v_{ij} = \sum_j \exp[(r_0 - r_{ij})/B]$ , where  $r_0$  is the bond-valence parameter (here  $r_0=1.905$  for  $\text{Sn}^{\text{IV}}\text{-O}$ ),  $r_{ij}$  is the bond length between atoms  $i$  and  $j$ ;  $B$  is a constant, the “universal parameter”  $\sim 0.37 \text{ \AA}$ ;  $v_{ij}$  is the valence of a bond between atoms  $i$  and  $j$ ;  $V_i$  is the sum of all bond valences of the bonds formed by a given atom  $i$ .<sup>[10]</sup>

**Table S3.** Crucial vertical excitation properties of **Sn<sub>18</sub>**

Transition	$\lambda_{\text{max}}$	$f$	Electronic transition
S0-S4	292	0.1588	H-2 -> L+11 51.3%, H-8 -> L+2 33.8%
S0-S22	258	0.1680	H-5 -> L+13 39.0%, H-5 -> L+1 21.8%, H-5 -> L+5 16.6%
S0-S23	257	0.1303	H-6 -> L+12 39.7%, H-6 -> L 27.8%, H-6 -> L+4 11.8%
S0-S26	248	0.3498	H-12 -> L+9 64.9%, H-12 -> L+4 7.5%, H-12 -> L+6 5.6%, H-16 -> L+9 5.0%
S0-S27	246	0.1650	H-10 -> L+10 64.1%, H-10 -> L+3 8.5%
S0-S30	244	0.1914	H-18 -> L+2 54.4%, H-22 -> L 14.4%
S0-S38	237	0.1367	H-21 -> L+5 33.6%, H-21 -> L+3 11.5%, H-5 -> L+1 11.5%, H-5 -> L+13 6.9%, H-2
S0-S40	236	0.1308	H-5 -> L+13 27.5%, H-5 -> L+1 25.5%, H-24 -> L+3 13.9%
S0-S41	235	0.2347	H-24 -> L+3 13.8%, H-11 -> L+11 10.2%, H -> L+7 6.5%, H-26 -> L+1 5.8%
S0-S42	235	0.5086	H-23 -> L+4 18.4%, H-6 -> L+12 9.4%, H -> L+7 8.0%, H-22 -> L+4 6.6%, H-26 -> L+1 6.4%, H-6 -> L 5.9%
S0-S43	234	0.1898	H -> L+7 7.5%, H-24 -> L+3 6.6%, H-21 -> L+5 6.6%, H-23 -> L+4 6.3%
S0-S47	232	0.1652	H-25 -> L+6 31.1%, H-2 -> L+3 10.4%
S0-S48	232	0.1685	H-25 -> L+6 5.5%, H-81 -> L 5.1%
S0-S57	228	0.5894	H-26 -> L+1 12.3%, H-17 -> L+7 11.1%, H-20 -> L+7 10.7%, H-9 -> L+7 7.1%, H-22 -> L+8 6.9%, H-9 -> L+1 5.0%

$\lambda_{\text{max}}$  and  $f$  are the maximum absorption wavelength and oscillation strength. H and L denote HOMO and LUMO, respectively.

**Table S4.** Interfragment charge transfer (IFCT) of main excited states for the **Sn<sub>18</sub>** wheel cluster.

main excited states	MLCT(metal to ligand charge transfer)	LLCT(ligand to ligand charge transfer)	LE (localized excitation)
S0-S4	5.0 %	0.5 %	94.5 %
S0-S22	2.0 %	0.5 %	97.5 %
S0-S23	2.0 %	0.4 %	97.6 %
S0-S26	1.4 %	0.3 %	98.3 %
S0-S27	1.5 %	0.1 %	98.4 %
S0-S30	6.0 %	7.0 %	87.0 %

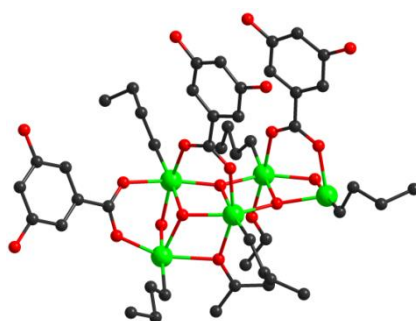


**Figure S1.** The asymmetric unit of **TOC-9**. Atom color code: green Sn; red O; black C.

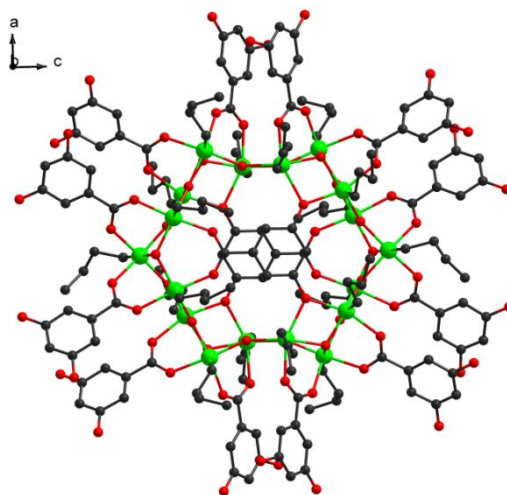


**Figure S2.** Ball-and-stick view of **TOC-9**. Atom color code: green Sn; red O; black C.

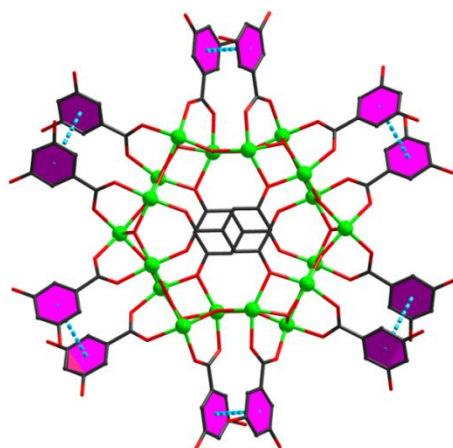


**Figure S3.** Illustration of the  $\pi$ - $\pi$  interactions of the decorating H<sub>2</sub>DBA ligands of TOC-9. Atom color code: green Sn. In order to clarify, the butyl groups are omitted.

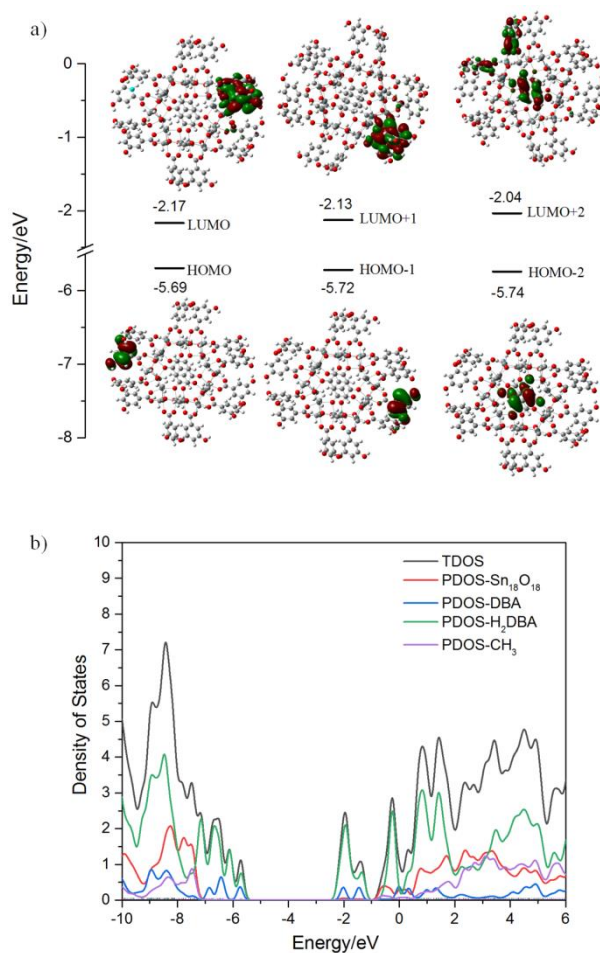


**Figure S4.** (a) Frontier molecular orbitals of Sn<sub>18</sub> wheel cluster. (b) Density of states (DOSs) and partial density of states (PDOSs) of Sn<sub>18</sub> wheel cluster. The black line represents the total DOSs, the blue, green and purple lines were PDOSs for Ligands (L) and red line was the PDOSs for Sn<sub>18</sub>O<sub>18</sub> cluster.

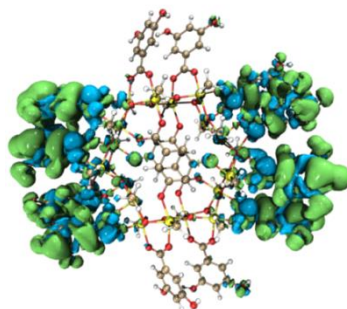


**Figure S5.** Third-order nonlinear static susceptibility density (isovalue = 200) of the **Sn<sub>18</sub>**.

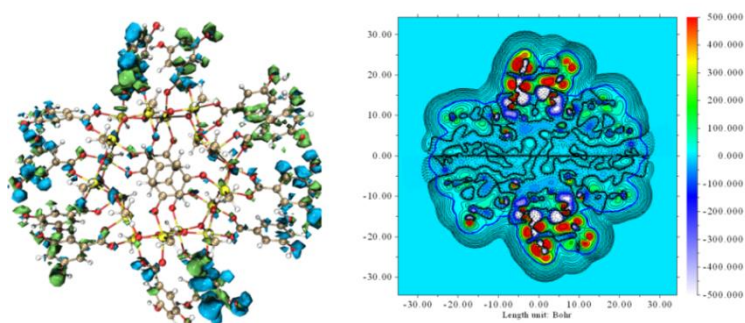


**Figure S6.** Third-order nonlinear static susceptibility density (isovalue = 200), xy plane of adding the electric field with 0.003, 0.006, -0.006, -0.003 a.u. in the y direction for the **Sn<sub>18</sub>**.

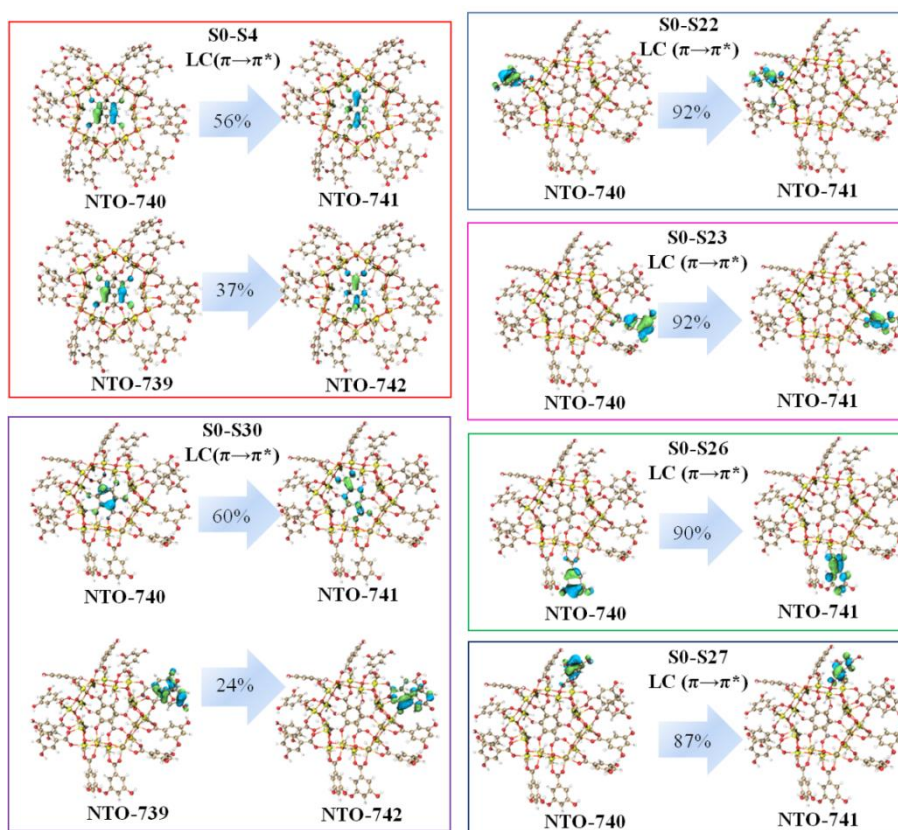


**Figure S7.** The natural transition orbitals (NTO) of **Sn<sub>18</sub>** wheel cluster.

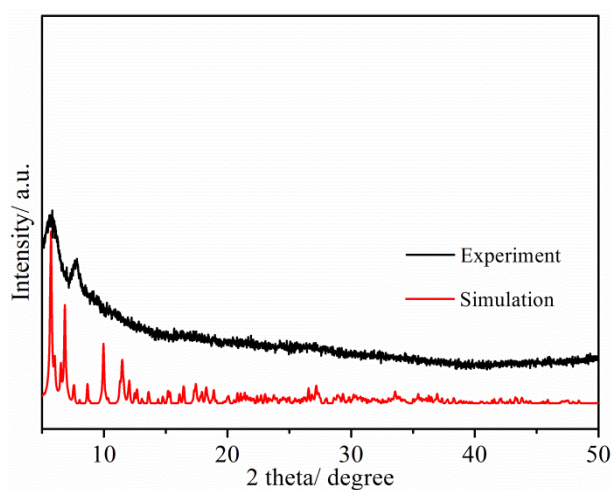


**Figure S8.** Simulated and experimental PXRD pattern of compound **TOC-9**.

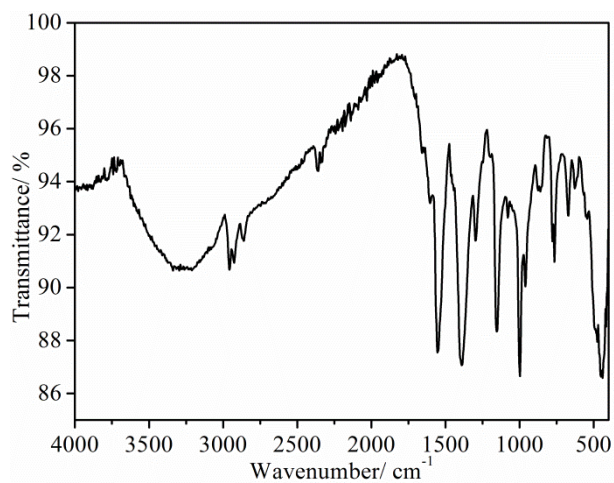


**Figure S9.** IR spectrum of compound **TOC-9**.

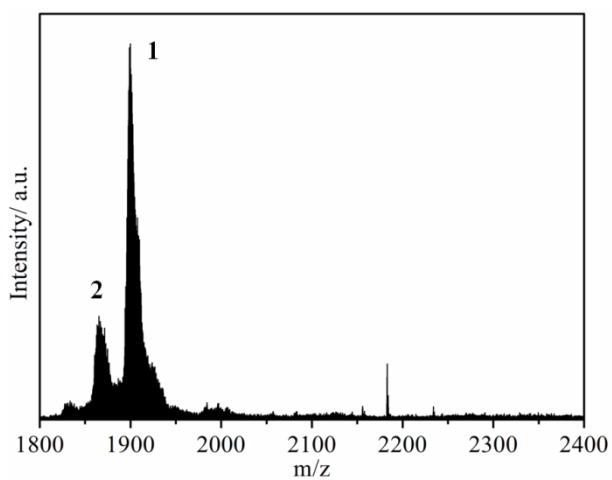


**Figure S10.** Negative-mode ESI-MS spectrum of **TOC-9** dissolved in acetonitrile.

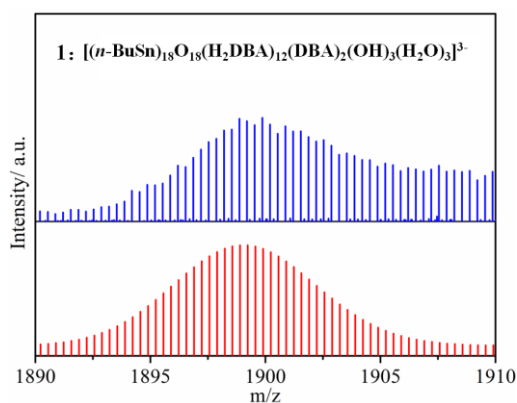


**Figure S11.** Experimental ESI-MS (-, blue spectrum) and calculated peak positions (red) for **TOC-9**.

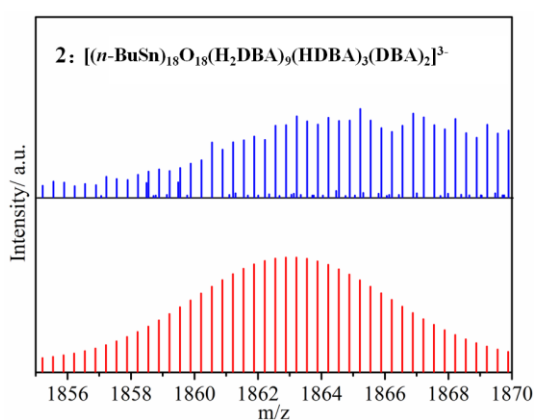


**Figure S12.** Experimental ESI-MS (-, blue spectrum) and calculated peak positions (red) for **TOC-9**.

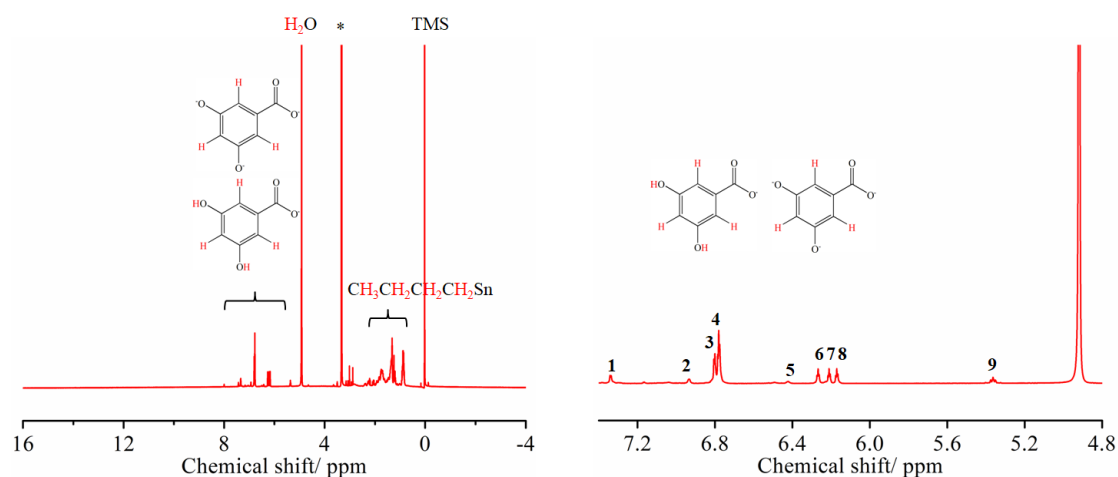


**Figure S13.**  $^1\text{H}$  NMR of **TOC-9** in  $\text{CD}_3\text{OD}$  (D, 99.8%) + 0.03% V/V TMS. The peak with an \* is due to solvent residual peak. Integration values for **TOC-9**: 1) 4.00 2) 2.00 3) 4.00 4) 8.01 5) 1.00 6) 3.99 7) 4.00 8) 4.01 9) 2.00. The peak of **1** was normalized to 4.00.

## References

- [1] M. J. Frisch, G. W. Trucks, H. B. Schlegel, G. E. Scuseria, M. A. Robb, J. R. Cheeseman, G. Scalmani, V. Barone, G. A. Petersson, H. Nakatsuji, X. Li, M. Caricato, A. V. Marenich, J. Bloino, B. G. Janesko, R. Gomperts, B. Mennucci, H. P. Hratchian, J. V. Ortiz, A. F. Izmaylov, J. L. Sonnenberg, D. Williams-Young, F. Ding, F. Lipparini, F. Egidi, J. Goings, B. Peng, A. Petrone, T. Henderson, D. Ranasinghe, V. G. Zakrzewski, J. Gao, N. Rega, G. Zheng, W. Liang, M. Hada, M. Ehara, K. Toyota, R. Fukuda, J. Hasegawa, M. Ishida, T. Nakajima, Y. Honda, O. Kitao, H. Nakai, T. Vreven, K. Throssell, J. J. A. Montgomery, J. E. Peralta, F. Ogliaro, M. J. Bearpark, J. J. Heyd, E. N. Brothers, K. N. Kudin, V. N. Staroverov, T. A. Keith, R. Kobayashi, J. Normand, K. Raghavachari, A. P. Rendell, J. C. Burant, S. S. Iyengar, J. Tomasi, M. Cossi, J. M. Millam, M. Klene, C. Adamo, R. Cammi, J. W. Ochterski, R. L. Martin, K. Morokuma, O. Farkas, J. B. Foresman, D. J. Fox, *Gaussian 16, revision C. 01*, Gaussian, Inc.: Wallingford CT, 2016.
- [2] P. J. Stephens, F. J. Devlin, C. F. Chabalowski, M. J. Frisch, *J. Phys. Chem.*, 1994, **98**, 11623.
- [3] S. Grimme, J. Antony, S. Ehrlich, H. Krieg, *J. Chem. Phys.*, 2010, **132**, 154104.
- [4] A. D. Becke, *J. Chem. Phys.*, 1993, **98**, 1372.
- [5] C. T. Lee, W. T. Yang, R. G. Parr, *Phys. Rev. B*, 1988, **37**, 785.
- [6] A. D. Becke, *Phys. Rev. A*, 1988, **38**, 3098.
- [7] W. R. Wadt, P. J. Hay, *J. Chem. Phys.*, 1985, **82**, 284.
- [8] P. J. Hay, W. R. Wadt, *J. Chem. Phys.*, 1985, **82**, 299.
- [9] P. J. Hay, W. R. Wadt, *J. Chem. Phys.*, 1985, **82**, 270.
- [10] T. Yanai, D. P. Tew, N. C. Handy, *Chem. Phys. Lett.*, 2004, **393**, 51.
- [11] T. Lu, F. Chen, *J. Comput. Chem.*, 2012, **33**, 580.
- [12] W. Humphrey, A. Dalke, K. Schulten, *J. Molec. Graphics*, 1996, **14**, 33.
- [13] F. Meyers, S. R. Marder, B. M. Pierce, J. L. Bredas, *J. Am. Chem. Soc.*, 1994, **116**, 10703.
- [14] G. M. Sheldrick, *Acta Crystallogr. C*, 2015, **C71**, 3.
- [15] A. L. Spek, *Acta Crystallogr. C*, 2015, **C71**, 9.
- [16] N. E. Brese, M. O'Keeffe, *Acta Crystallogr. B*, 1991, **B47**, 192.